NACA

RESEARCH MEMORANDUM

FREE-FLIGHT INVESTIGATION AT

MACH NUMBERS FROM 0.8 TO 1.5 OF THE EFFECT OF

A FUSELAGE INDENTATION ON THE ZERO-LIFT DRAG

OF A 52.5° SWEPTBACK-WING—BODY CONFIGURATION

WITH SYMMETRICALLY MOUNTED STORES

ON THE FUSELAGE

By Sherwood Hoffman

Langley Aeronautical Laboratory
Langley Field, Va.

NATIONAL ADVISORY COMMITTEE
FOR AERONAUTICS

WASHINGTON
February 20, 1958

T62-19223-DD

T58-4892

DECLASSIFIED CONFIDENTIAL

NATIONAL ADVISORY COMMITTEE FOR AERONAUTICS

RESEARCH MEMORANDUM

FREE-FLIGHT INVESTIGATION AT

MACH NUMBERS FROM 0.8 TO 1.5 OF THE EFFECT OF

A FUSELAGE INDENTATION ON THE ZERO-LIFT DRAG

OF A 52.5° SWEPTBACK-WING—BODY CONFIGURATION

WITH SYMMETRICALLY MOUNTED STORES

ON THE FUSELAGE

By Sherwood Hoffman

SUMMARY

Two rocket-propelled models were flight-tested at Mach numbers from 0.8 to 1.5 to determine the effect of a fuselage indentation on the drag of a 52.5° sweptback-wing—body configuration with two large strut-mounted stores symmetrically located above and below the fuselage. The fuselage had a symmetrical, Mach number 1.0 indentation designed to cancel the wing area normal to the plane of symmetry. The indentation reduced the total drag of the configuration at high subsonic and low supersonic speeds but increased the total drag at Mach numbers above 1.28. The agreement obtained between the measured and theoretical (supersonic area rule) pressure drags ranged from good for the models without stores to poor for the models with stores.

INTRODUCTION

This paper presents the results of a free-flight investigation which was conducted to determine the effect of a fuselage indentation on the zero-lift drag of a sweptback-wing—body configuration with a relatively large store mounted below the fuselage. The fuselage was indented symmetrically to cancel only the wing cross-sectional areas normal to the axis of symmetry in order to minimize the sonic drag rise (ref. 1) of the wing-body combination. The store was strut-mounted parallel to the body axis in the region of the indentation and in a
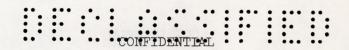
CONFIDENTIAL

T58-4892

plane perpendicular to the wing plane. A second store was mounted on the opposite side of the fuselage in order to make the model symmetrical and thereby to maintain flight at zero lift. In a previous investigation (ref. 2), the effect on drag of mounting a partially submerged store in the region of the fuselage indentation was determined for this same wing-body combination. Reference 3 presents the effect of a similar fuselage indentation on the drag of a sweptback-wing—body configuration with external stores tested in various positions on the wing.

The configurations were rocket-propelled vehicles tested through a range of Mach number from 0.8 to 1.5 and corresponding Reynolds number, based on wing mean aerodynamic chord, from about 5×10^6 to 14×10^6. The comparisons presented include data from previous tests (refs. 4 and 5) and theoretical pressure drags that were computed by using the linearized, supersonic area-rule theory of reference 6.

SYMBOLS

A cross-sectional area, sq ft

a longitudinal acceleration, ft/sec^2

C_D total-drag coefficient, based on S_w

$C_{D,f}$ friction-drag coefficient

ΔC_D pressure-drag coefficient, $C_D - C_{D,f}$

g acceleration due to gravity, $32.2 \ ft/sec^2$

L length of fuselage, ft

M free-stream Mach number

q free-stream dynamic pressure, lb/sq ft

R Reynolds number, based on wing mean aerodynamic chord

S_w total wing plan-form area, sq ft

W weight, lb

DECLASSIFIED

x   station measured from fuselage nose, ft

γ elevation angle of flight path, deg

MODELS

A list of the models tested, including six models used in the investigations of references 4 and 5, and their designations are given in table I. Details and dimensions of the wing-body-store configurations are presented in figure 1 and tables II to VI. The normal cross-sectional-area distributions and photographs of the models are shown in figures 2 and 3, respectively.

All the models were symmetrical configurations for the zero-lift attitude. Model A consisted of a 52.5° sweptback wing, a parabolic fuselage, a pair of strut-mounted stores that were attached separately above and below the fuselage, and four stabilizing fins as is shown in figure 1(a). The fuselage was formed from two parabolas of revolution joined at the maximum diameter (40-percent station) and had an overall fineness ratio of 10. The wing, which was mounted symmetrically about the body center line, had an angle of sweepback of 52.5° along the quarter-chord line, a total aspect ratio of 3.0, a taper ratio of 0.2, and an NACA 65A004 airfoil section in the free-stream direction. The stores had a fineness ratio of 8.57, a length equal to 1.16 times the length of the wing mean aerodynamic chord, and four equally spaced fins. The stores were 0.10-scale models of the 150-gallon Douglas Aircraft Company store (ref. 7). The center of gravity of each store was located longitudinally at the 52.5-percent fuselage station and the minimum vertical distance between the store and fuselage was 0.333 of the maximum store diameter. The 6-percent-thick strut was similar to the Douglas three-hook shackle pylon of reference 8. The ratio of frontal area of the two stores to the wing plan-form area was 0.0126 and the ratio of the fuselage frontal area to the wing plan-form area was 0.0606.

Model B was identical to model A except for the body indentation. The fuselage was indented symmetrically (according to the transonic area rule of ref. 1) to cancel only the exposed-wing cross-sectional areas normal to the axis of symmetry. There was no incidence between the stores, wings, and fuselages of the configurations.

Models C, D, E, G, and the isolated store were tested originally for the investigations of references 4 and 5. These models correspond to the wing and parabolic body, wing and indented body, parabolic body alone, the parabolic body with a pair of strut-mounted stores, and the

isolated store. (See table I.) Model F, which was tested as part of
the present investigation, was the indented fuselage alone.

TEST TECHNIQUE

All the models were tested at the Langley Pilotless Aircraft Research
Station at Wallops Island, Va. Each model was boosted from a zero-length
launcher to supersonic speeds by a fin-stabilized 6-inch ABL Deacon rocket
motor. Model B and the booster in the launching position are shown in
figure 3(c). After burnout of the booster rocket fuel, the higher drag-
weight ratio of the booster as compared with that of the model allowed
the model to separate longitudinally from the booster. Velocity and
trajectory data were obtained from the CW Doppler velocimeter and the
NACA modified SCR-584 radar tracking unit, respectively. A survey of
atmospheric conditions including winds aloft was made from an ascending
balloon that was released at the time of each launching.
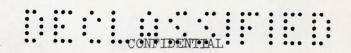
DATA REDUCTION AND ANALYSIS

All data were recorded during coasting flight as the models, free
from their boosters, decelerated through the Mach number ranges reported.
The zero-lift, total-drag coefficient of each model was evaluated from
the expression

$$C_D = - \frac{W}{g q S_W} \left[a + g \sin \gamma \right]$$

where a was obtained by differentiating the velocity-time curve
obtained from the velocimeter. The values of q and γ were obtained
from the measurements of tangential velocity and atmospheric conditions
along each trajectory.

The error in total-drag coefficient, based on S_W, was estimated
to be less than ±0.0007 at supersonic speeds and ±0.0010 at subsonic
speeds. The Mach numbers were determined within ±0.01 throughout the
test range.

The experimental pressure-drag coefficient was obtained by sub-
tracting an estimated total friction-drag coefficient and the pressure-
drag coefficient of the four stabilizing fins from the total-drag coef-
ficient at corresponding Mach numbers. The friction drag through the
Mach number range was determined by adjusting the experimental subsonic

drag level of each model for Reynolds number effect with the use of the equations of Van Driest (ref. 9). Also, it was assumed that the boundary layer over the fuselage and stores was altogether turbulent and that transition occurred at the 30-percent-chord station of the wing and at the 50-percent-chord station of the struts and fins. The drag of the stabilizing fins, which was obtained from reference 10, was assumed to be the same on all models tested. No adjustments were made for the base drag rise of any of the models. Reference 10, however, indicates that for afterbodies similar to those used herein, the base drag rise is of the order of accuracy of the drag measurements and may be neglected.

The theoretical pressure drags were computed by using the supersonic area-rule theory of reference 6. The computational procedure is described in reference 11. Since the models were symmetrical, only the projected area distributions between 0° and 90° of roll of the model with respect to the inclined Mach planes had to be considered. The area distributions of the models (neglecting stabilizing fins) were determined graphically (see ref. 12) and corresponded to roll angles of 0°, 22.5°, 45°, 67.5°, and 90° at $M = 1.5$. It had been assumed that a cylinder can be added to the base of each model without altering the drag. If this assumption were not made, the solution would require the flow to fill the area behind the base and would exceed the limitations of the linearized theory. The Fourier series used for calculating the pressure drag were evaluated for 33 harmonics, and plots of these series indicated that they were convergent.

RESULTS AND DISCUSSION

The Reynolds number and Mach number ranges of the models tested in the present investigation and in the investigations of references 4 and 5 are presented in figure 4. The present models were tested through a range of Mach number from about 0.8 to 1.5 with corresponding Reynolds number from approximately 5×10^6 to 14×10^6 based on wing mean aerodynamic chord. Except for the isolated store, the Reynolds numbers for the models of references 4 and 5 are of the same magnitude as those of the present tests at corresponding Mach numbers.
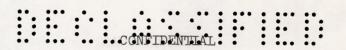
Total Drag

Figure 5 presents a comparison of the zero-lift, total-drag coefficients and friction-drag coefficients of the two wing-body-store models. Indenting the fuselage (model B) to cancel only the wing cross-sectional areas reduced the total drag of the configuration at high subsonic and low supersonic speeds. The 0.001 reduction in C_D near $M = 0.9$ is

due almost entirely to the difference in skin friction of the models.
At M = 1.1 the drag reduction due to the indentation is only slightly
larger than the reduction obtained at subsonic speeds. The comparison
also shows that the transonic (M = 1.0) indentation used is ineffective
above M = 1.28 and results in more total drag than was obtained from
the unindented model. In view of the smaller volume of model B rela-
tive to model A (24 percent less fuselage volume) and the limited range
of Mach number through which the indentation reduced C_D, it appears
that the indented model with stores has no drag advantage over the
unindented model with stores.

A breakdown of the drags of models A and B is presented in fig-
ures 6 and 7, respectively. For the unindented configurations
(fig. 6(a)), the interference between the wing, fuselage, and stores
appears to be negligible through most of the Mach number range. A com-
parison of the drag increments between models G and E with the drag of
the isolated stores in figure 6(a) shows that the interference between
the store and fuselage (neglecting wings) is approximately zero at all
test Mach numbers. When the wing is added, the interference effects
are altered only slightly as may be seen by comparing the incremental
drags between models A and C with those between models G and E. This
result would be expected for the present symmetrical models, since the
thin wing tends to act as a reflection plane (ref. 13) and, as a result,
does not alter the flow field about the configuration appreciably. When
the fuselage is indented to cancel the wing cross-sectional areas
(fig. 7(a)), the store-plus-interference drag increases markedly at
transonic and supersonic speeds. A comparison of the incremental drags
between models B and D with that of the isolated stores shows that the
interference drag due to adding the stores to the indented configuration
varies from 30 percent to 100 percent of the isolated store drag between
Mach numbers 1.0 and 1.5. The increase in interference relative to the
unindented configuration with stores may be explained by the increased
suction forces acting on the store afterbody due to the flow expanding
into the region of the indentation. Also, the suction pressures from
the store afterbody result in a higher interference drag when they act
on the steeper body slopes of the indented body than on the lower body
slopes of the parabolic body.

The effect of the indentation on the wing-plus-interference drag
also may be seen in figures 6 and 7. The incremental drag between
models C and E (fig. 6(a)) shows that the wing of the unindented con-
figuration has a drag coefficient of about 0.004 at subsonic speed,
0.006 near M = 1.0, and about 0.008 at supersonic speeds. A comparison
of these values with the wing-plus-interference drag of the indented
configuration (increment between models D and F in fig. 7(a)) shows
that the transonic indentation effectively cancelled the wing drag near
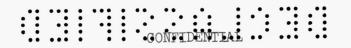M = 1.0 and produced a significant reduction in the incremental wing

DECLASSIFIED

drag at the other test Mach numbers. For the present case, the indentation produced favorable interference effects near M = 1.0 of such magnitude as to cancel the wing friction drag as well as its pressure drag. These gains were partly offset by the fact that the indentation increased the drag of the fuselage.

Pressure Drag

The theoretical pressure drags of the models tested are compared with the experimental pressure drags in figures 8 and 9. The friction-drag curves, which were subtracted from the total-drag curves to give ΔC_D, are presented in part (b) of figures 6 and 7.

The comparisons in figures 8 and 9 show that the agreement between the supersonic area-rule theory and experiment ranged from good for the models without stores to poor for the models with stores. The least agreement was for model B where the theoretical values near M = 1.3 were about 30 percent lower than the experimental values. This difference or error is about twice as great as the pressure drag of the isolated stores. In references 3, 14, and 15, where stores (or nacelles) were tested on wings of configurations having fuselage indentations, the agreement between theory and experiment also varied erratically from good to poor. It is evident that the area rule, which is linearized theory, cannot account for all the interference effects, especially local interference effects. From a qualitative aspect, however, the theory indicates a reduction in pressure drag due to the indentation on the present wing-body combination with and without the stores at transonic speeds (fig. 8) as well as the decreasing effectiveness of the indentation with increasing Mach number. The comparison of the normal cross-sectional-area distributions in figure 2 indicates only the relative ΔC_D levels of the models near M = 1.0. Adding the stores to either the indented or unindented body-wing combination results in a more bumpy area distribution and higher pressure drag.

The pressure drags of the models having equal normal cross-sectional-area distributions are compared in figure 9. The pressure drags of the models with equal areas agree within 15 percent at M = 1.0 and diverge with increasing Mach number. The supersonic area-rule (theoretical) values, shown in figure 9, also diverge with increasing Mach number for the identical normal area models, but underestimate the magnitude of the changes by approximately half of the measured amounts.

CONCLUDING REMARKS

The effect of a Mach number 1.0 indentation on the drag of a 52.5°
sweptback wing-body configuration with two large stores located symmet-
rically above and below the fuselage was determined by free-flight tests
between Mach numbers of 0.8 and 1.5. Indenting the fuselage for the
wing alone reduced the configuration total drag at high subsonic and low
supersonic speeds, and increased the total drag above Mach number 1.28.
The stores were located in the region of the body indentation and
experienced unfavorable interference effects through most of the Mach
number range. The agreement between the measured pressure drags and
those calculated from supersonic area-rule theory ranged from good for
models without stores to very poor for models with stores, in which
case the difference between experiment and theory was as much as 30 per-
cent. Although the theoretical drag levels corresponded to the measured
levels, the theory does not account for all the interference effects,
especially local effects.

Langley Aeronautical Laboratory,
       National Advisory Committee for Aeronautics,
              Langley Field, Va., November 15, 1957.

REFERENCES

1. Whitcomb, Richard T.: A Study of the Zero-Lift Drag-Rise Characteristics of Wing-Body Combinations Near the Speed of Sound. NACA Rep. 1273, 1957. (Supersedes NACA RM L52H08.)

2. Hoffman, Sherwood: Zero-Lift Drag of a Large Fuselage Cavity and a Partially Submerged Store on a 52.5° Sweptback-Wing—Body Configuration As Determined From Free-Flight Tests at Mach Numbers of 0.7 to 1.53. NACA RM L56L21, 1957.

3. Pearson, Albin O.: Transonic Investigation of Effects of Spanwise and Chordwise External Store Location and Body Contouring on Aerodynamic Characteristics of 45° Sweptback Wing-Body Configurations. NACA RM L57G17, 1957.

4. Hoffman, Sherwood, and Wolff, Austin L.: Effect on Drag of Longitudinal Positioning of Half-Submerged and Pylon-Mounted Douglas Aircraft Stores on a Fuselage With and Without Cavities Between Mach Numbers 0.9 and 1.8. NACA RM L54E26, 1954.

5. Hoffman, Sherwood: A Flight Investigation of the Transonic Area Rule for a 52.5° Sweptback Wing-Body Configuration at Mach Numbers Between 0.8 and 1.6. NACA RM L54H13a, 1954.

6. Jones, Robert T.: Theory of Wing-Body Drag at Supersonic Speeds. NACA Rep. 1284, 1956. (Supersedes NACA RM A53H18a.)

7. Muse, T. C., and Kasri, E. B.: Wind Tunnel Tests of the Douglas Aircraft Store With Various Fins. Rep. No. ES 21198, Douglas Aircraft Co., Inc., July 15, 1948.

8. Dugan, James C.: External Store Development. Memo. Rep. No. WCNSR-43019-1-1, Wright Air Dev. Center, U. S. Air Force, Aug. 13, 1951.

9. Van Driest, E. R.: Turbulent Boundary Layer in Compressible Fluids. Jour. Aero. Sci., vol. 18, no. 3, Mar. 1951, pp. 145-160, 216.

10. Morrow, John D., and Nelson, Robert L.: Large-Scale Flight Measurements of Zero-Lift Drag of 10 Wing-Body Configurations at Mach Numbers From 0.8 to 1.6. NACA RM L52D18a, 1953.

11. Holdaway, George H.: Comparison of the Theoretical and Experimental Zero-Lift Drag-Rise Characteristics of Wing-Body-Tail Combinations Near the Speed of Sound. NACA RM A53H17, 1953.

12. Nelson, Robert L., and Welsh, Clement J.: Some Examples of the
    Applications of the Transonic and Supersonic Area Rules to the
    Predictions of Wave Drag. NACA RM L56D11, 1956.

13. Smith, Norman F., and Carlson, Harry W.: The Origin and Distribu-
    tion of Supersonic Store Interference From Measurement of
    Individual Forces on Several Wing-Fuselage-Store Configurations.
    I.- Swept-Wing Heavy-Bomber Configuration With Large Store
    (Nacelle). Lift and Drag; Mach Number 1.61. NACA RM L55A13a, 1955.

14. Hoffman, Sherwood: Free-Flight Investigation of the Drag of a Model
    of a 60° Delta-Wing Bomber With Strut-Mounted Siamese Nacelles and
    Indented Fuselage at Mach Numbers From 0.80 to 1.35. NACA
    RM L57G29, 1957.

15. Petersen, Robert B.: Comparison of the Experimental and Theoretical
    Zero-Lift Wave-Drag Results for Various Wing-Body-Tail Combinations
    at Mach Numbers Up to 1.9. NACA RM A56I07, 1957.

12. Nelson, Robert L., and Welsh, Clement J.: Some Examples of the Application of the Transonic and Supersonic Area Rules to the Prediction of Wave Drag. NACA RM L56D11, 1956.

13. Smith, Norman F., and Carlson, Harry W.: The Origin and Distribution of Supersonic Store Interference From Measurement of Individual Forces on Several Wing-Fuselage-Store Configurations. I.- Swept-Wing Heavy-Bomber Configuration With Large Store. (Bodies of Fineness Ratio 7). NACA RM L55A13a, 1955.

14. Hoffman, Sherwood: Free-Flight Investigation of the Drag of a Nonlifting 60° Delta-Wing Body Combination as Influenced by Inlets and Inlet Fences. NACA RM L56A19, 1956.

15. Hoffman, Sherwood: Comparison of Theoretical and Experimental Store Drag. NACA RM L55J10, 1955.

TABLE I.- MODELS

Model	Description
A	Wing + parabolic body + 2 stores
B	Wing + indented body + 2 stores
C	Wing + parabolic body (ref. 5)
D	Wing + indented body (ref. 5)
E	Parabolic body (ref. 5)
F	Indented body
G	Parabolic body + 2 stores (ref. 4)
-	Isolated store (ref. 4)

TABLE II.- COORDINATES OF NACA 65A004 AIRFOIL

Station, percent chord	Ordinate, percent chord
0	0
.5	.311
.75	.378
1.25	.481
2.5	.656
5.0	.877
7.5	1.062
10.00	1.216
15.00	1.463
20.00	1.649
25.00	1.790
30.00	1.894
35.00	1.962
40.00	1.996
45.00	1.996
50.00	1.952
55.00	1.867
60.00	1.742
65.00	1.584
70.00	1.400
75.00	1.193
80.00	.966
85.00	.728
90.00	.490
95.00	.249
100.00	.009
L. E. radius: 0.102 T. E. radius: 0.010	

DECLASSIFIED CONFIDENTIAL

TABLE III.- COORDINATES OF PARABOLIC BODY

[Stations measured from body nose]

Station, in.	Ordinate, in.
0	0
1	.245
2	.481
4	.923
6	1.327
10	2.019
14	2.558
18	2.942
22	3.173
26	3.250
30	3.233
34	3.181
38	3.095
42	2.975
46	2.820
50	2.631
54	2.407
58	2.149
62	1.857
65	1.615

TABLE IV.- COORDINATES OF BODY WITH INDENTATION

[Stations measured from body nose]

Station, in.	Ordinate, in.
(a)	(a)
28	3.246
30	3.176
32	3.073
34	2.934
36	2.748
38	2.619
40	2.455
42	2.341
44	2.262
46	2.243
48	2.238
50	2.297
52	2.292
54	2.251
56	2.221
58	2.149
60	2.007
62	1.857
64	1.698
65	1.615

(a) Coordinates between stations 0 and 28 are identical to those of the parabolic body (table III).

CONFIDENTIAL
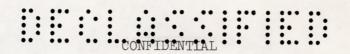
TABLE V.- COORDINATES OF STORE

[Stations measured from store nose]

Station, in.	Ordinate, in.
0	0
.35	.170
.85	.366
1.35	.517
1.85	.633
2.35	.723
2.85	.795
3.85	.905
4.85	.987
5.85	1.041
7.65	1.050
9.45	1.046
10.45	1.016
11.45	.960
12.45	.880
13.45	.780
14.45	.665
15.45	.538
16.45	.404
17.25	.293
17.65	.217
18.00	0
Trailing-edge radius, 0.100	

CONFIDENTIAL
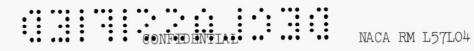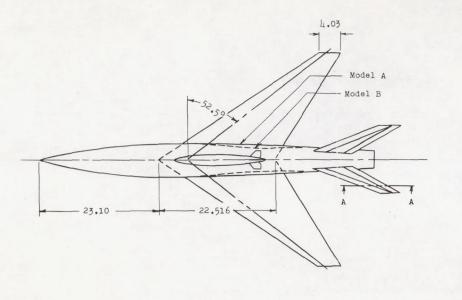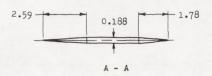
TABLE VI.- COORDINATES OF STRUT SECTION

[Stations measured from leading edge]

Station, in.	Ordinate, in.
0	0
.005	.016
.020	.030
.060	.051
.100	.065
.200	.090
.400	.120
.600	.137
.800	.147
1.001	.150
3.751	.150
5.000	0
Trailing-edge radius, 0.019	

Model A
Model B

4.03

52.50

23.10   22.516

A   A
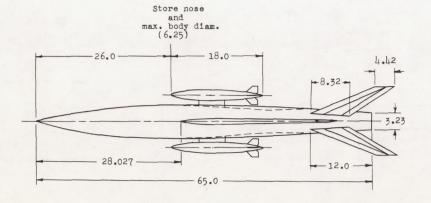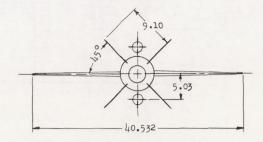
Model Characteristics

Wing aspect ratio..................... 3.0
Wing taper ratio...................... 0.2
Wing mean aerodynamic chord, ft..... 1.293
Free-stream airfoil............. NACA 65A004
Sweepback angle of quarter chord.... 52.5°
Total wing planform area, sq ft..... 3.802
Total exposed fin area, sq ft....... 1.332
Body fineness ratio................. 10.0
Body frontal area, sq ft............ 0.230
Store fineness ratio................ 8.570
Total store frontal area, sq ft..... 0.048
Strut thickness ratio............... 0.060
Sweepback angle of fuselage fins.... 60.0°

2.59   0.188   1.78

A - A

Typical fin section

Store nose
and
max. body diam.
(6.25)

26.0   18.0

4.42

8.32

3.23

28.027

12.0

65.0

9.10

45°

5.03

40.532
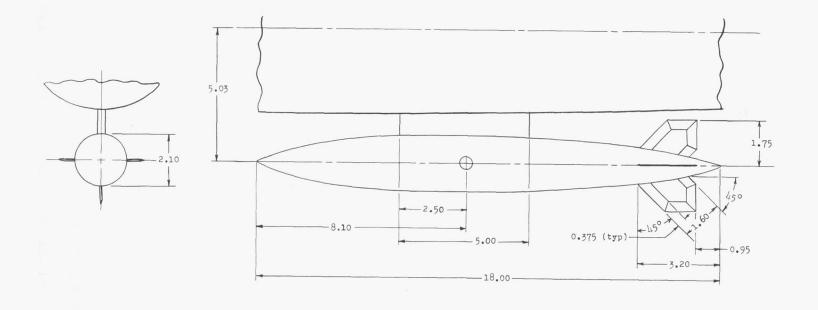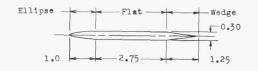
(a) Models A and B.

Figure 1.- Details and dimensions of the wing-body-store models.   Dimensions are in inches.

5.03

2.10

1.75

45°

1.60

45°

0.375 (typ)

0.95

2.50

8.10

5.00

3.20

18.00

Ellipse — Flat — Wedge

0.30

1.0   2.75   1.25

Store fineness ratio............. 8.570
Store frontal area, sq ft......... .024
Strut thickness ratio............. .060
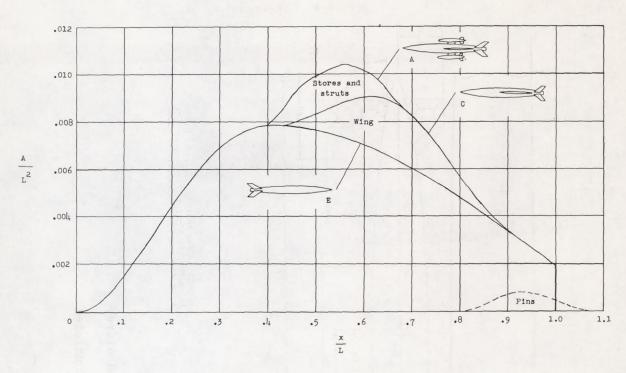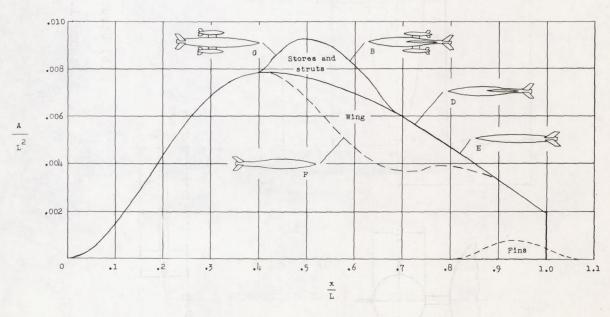
(b) Strut and store.

Figure 1.- Concluded.

DECLASSIFIED
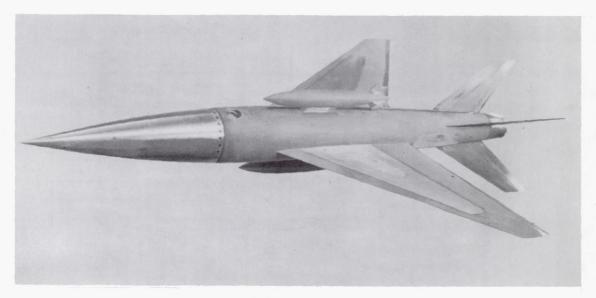
(a) Models A, C, and E.
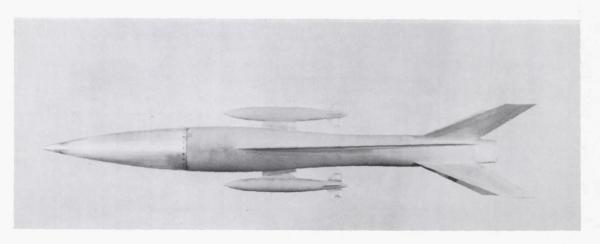
(b) Models B, D, E, F, and G.

Figure 2.- Normal cross-sectional-area distributions of models tested.

(a) Model A.

(b) Model B.   L-57-4441

Figure 3.- Views of models A and B.

DECLASSIFIED

(c) Model B and booster on zero-length launcher. L-87686

Figure 3.- Concluded.
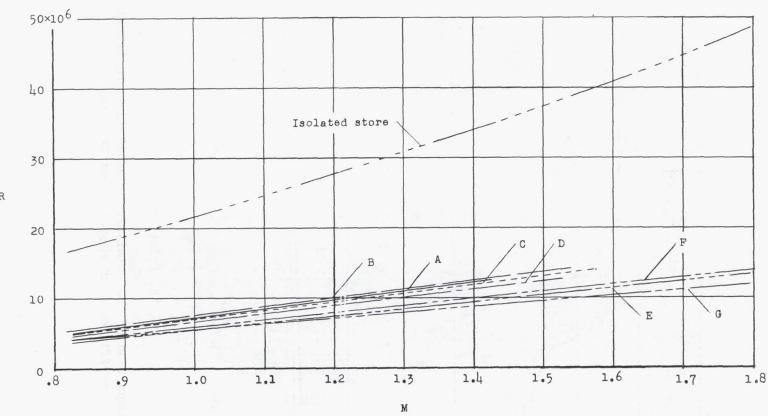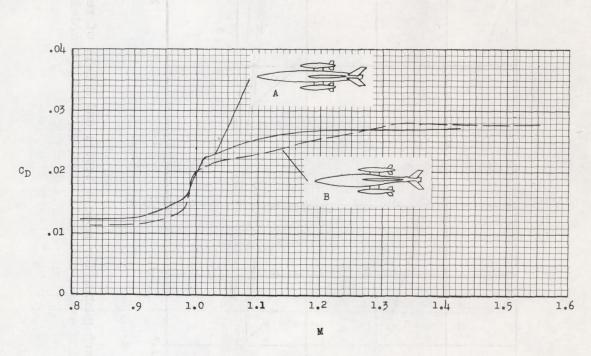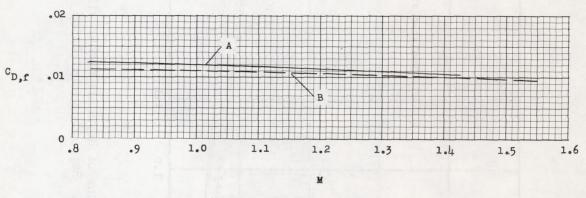
Figure 4.- Variations of Reynolds number with Mach number for models tested and models of ref-
erences 4 and 5. Reynolds number based on wing mean aerodynamic chord adjusted for model
scale.

(a) Total drag.
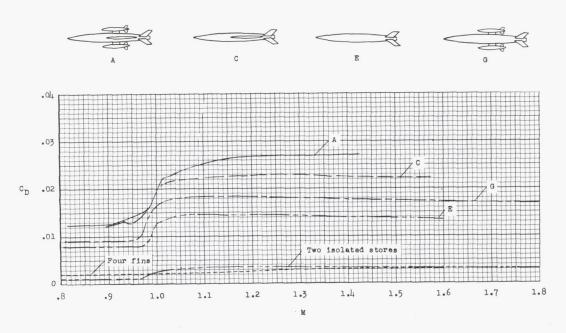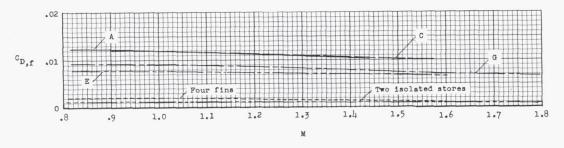
(b) Friction drag.

Figure 5.- Comparison of the total-drag coefficients and friction-drag coefficients of wing- body-store models.

(a) Total drag.
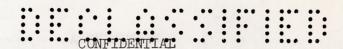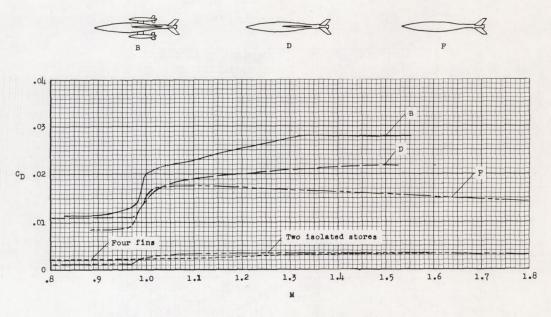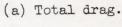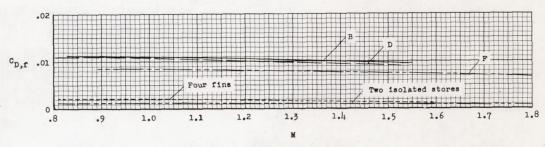
(b) Friction drag.

Figure 6.- Comparisons of total-drag coefficients and friction-drag coefficients of models with original, parabolic fuselage.
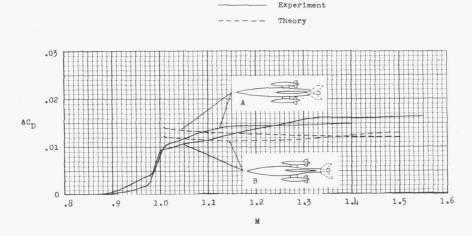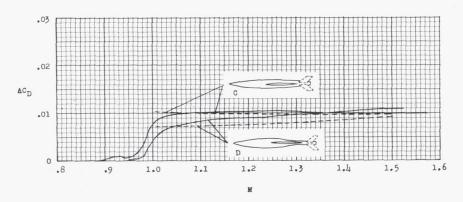
(a) Total drag.

(b) Friction drag.

Figure 7.- Comparisons of total-drag coefficients and friction-drag
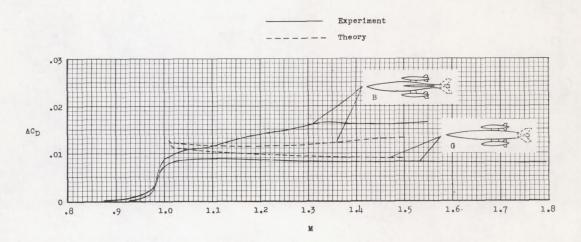coefficients of the models with indented fuselage.
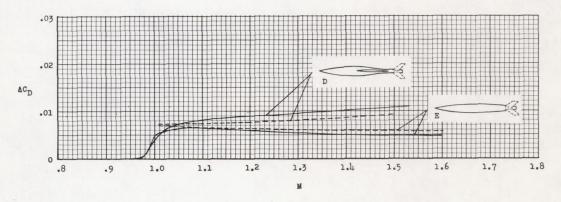
(a) Wing-body-store models.

(b) Wing-body models.

Figure 8.- Effect of fuselage indentation on measured and
theoretical pressure drags.

Experiment
Theory

ΔC_D

B

G

M

(a) Wing-body-store models.

ΔC_D

D

E

M

(b) Wing-body models.

Figure 9.- Comparisons of the measured and theoretical pressure drags for models having identical normal cross-sectional-area distributions.